# Modelling of Pulsed Eddy Current Testing of wall thinning of carbon steel pipes through insulation and cladding

S Majidnia[a,b], J Rudlin [a], R. Nilavalan [b]
[a] TWI Ltd, Granta Park Cambridge , [b] Brunel University London

**Abstract**

Conventional eddy current techniques have been used to a great extent for detection of surface breaking defects in conductive materials. Pulsed Eddy Current (PEC) techniques excite the probe's driving coil with a repetitive broadband pulse, usually a square wave, instead of sinusoidal wave. The resulting transient current through the coil induces transient eddy currents in the test piece, these pulses consist of a broad frequency spectrum, and the reflected signal contains important depth information.

Surface pancake type pulsed eddy current probes have been used for wall thinning and corrosion detection but these methods can be slow. In order to increase the scanned area, an encircling coil has been proposed, with a view to inspect a complete circumference with a single pulse. The work presented in this paper employs COMSOL Multiphysics finite element (FE) modelling software, to further investigate the behaviour of an encircling probe design as a part of the development work.

This work involves modelling of an encircling coil around a steel pipe with insulation and cladding of different materials. Pulsed eddy current testing of wall-thinning through cladding and insulation was studied for various wall thinning situations. The simulation results show the capability of this system in pipe wall thinning detection.

**Keywords:** Finite Element Analysis, Pulsed Eddy Current, Encircling Probe

# 1 Introduction

Pipes are widely used for transportation and distribution in power generation, oil and gas, chemical, and other related industries. Most of the pipes used under high temperature and high pressure conditions are made of ferromagnetic carbon steel, thermally insulated and externally protected by covering sheets made of aluminium alloy, stainless steel, or galvanized steel [1]. Over long period of service, corrosion may occur on the outer side of a pipe as corrosion under insulation (CUI) and result in wall-thinning which if not detected and treated might lead to a catastrophe. Regular monitoring of potential wall thinning by measuring the remaining wall thickness is necessary. Considering accessibility, safety, and efficiency, non-destructive testing without removing covering sheet and insulation layer is preferred. Eddy current method is a non-contact electromagnetic technique which has been used for decades in examination of pipes [2]. Pulsed eddy current testing (PECT) uses broad-band excitation for electromagnetic penetration into test objects. The PECT signal changes over time along with the penetration of eddy current and therefore it might be possible to characterize a test object from the analysis of the time-varying signal [3]. As the power consumed by short duty cycle pulses is lower than that of its sinusoidal counterpart with the same large excitation current, higher excitation pulses can be employed to strengthen induced eddy currents [4]. Fundamental studies have been undertaken extensively on analytical and numerical solutions of PECT for conductive plates [1] [5] [6] [7]. However studies in use of encircling probe and possible advantages of it over a surface type probe has not been considered. In this paper numerical modelling is used to investigate the use of an encircling probe in detection of corrosion and wall thinning under insulation.

The Finite Element Analysis for coated pipework introduces difficulties in computation, since not only the pipe but also the coating and covering with its length much larger than its thickness needs to be modelled. Solving a 3D model of such geometries result in a huge number of triangular mesh elements and make the subsequent calculation unlikely to succeed [8]. In the effort to overcome these difficulties 2D axisymmetric models are more preferable to study the problems related to coated pipework.

Three of the most commonly used coverings in oil and gas industries, aluminium, galvanized steel and stainless steel [1] are studied. The FEA of the PEC system described in this paper was developed using the commercial FEA package, COMSOL to find the response signal to uniform wall thinning.

## 1.1 ***Model setup***

The cross section of the coil around a pipe with covering and thermal insulation is schematically illustrated in Figure 1. An encircling probe consisting of an excitation coil and detection sensors was positioned outside of the pipe with nonconductive insulation and conductive covering as shown in Figure 1 (a). For PEC investigations of wall thinning under insulation 2D axisymmetric models were developed. A general schematic of the model used is shown in Figure 1 (b). The model consisted of an air domain which contained all of the geometries. Rectangular domains were used for pipe and covering and points were used as sensors in the model. Driver coil parameters and dimensions of the geometries used in the modelling can be found in Table 1 and Table 2. Geometry dimensions of the modelTable 2 respectively.

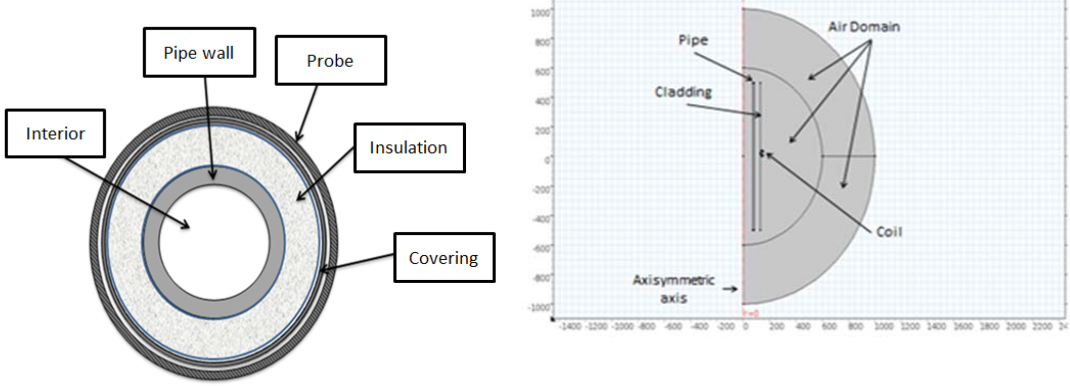


**Figure 1. a) Schematics of the probe around the pipe and insulation b) 2D axisymmetric model geometry**

**Table 1. Driver coil parameters**

| Driver coil parameters | |
|---|---|
| Number of turns | 10 |
| Coil Diameter | 268 [mm] |
| Wire conductivity | $6\times10^{7}$ [S/m] |
| Wire Diameter | 8[mm] |

**Table 2. Geometry dimensions of the model**

| Type | Outside diameter [mm] | Thickness [mm] | Lentgh [mm] |
|---|---|---|---|
| Pipe | 84 | 14 | 1000 |
| Covering | 261 | 0.7 | 1000 |
| Coil | 150 | 16 | 40 |
| Insulation | 260 | 46 | 1000 |
| Air | 4000 | 400 | -- |

Coil current input in time domain is shown in Figure 2.

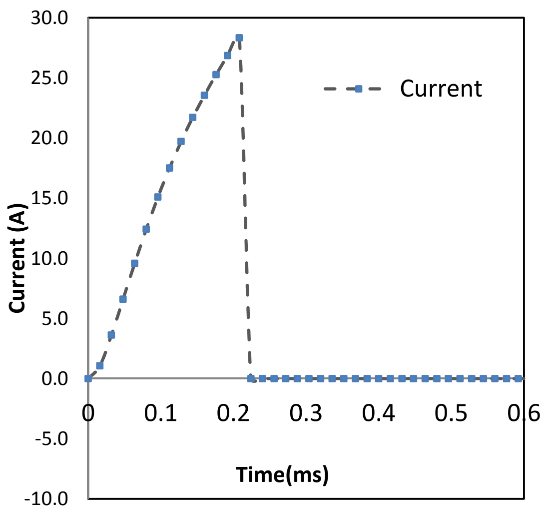


**Figure 2. a) Time domain current input in the model**

The induced current density on the pipe surface will follow a Lorentzian shape, with its maximum directly under the inductor. Figure 3 illustrates the magnetic field generated by the coil when pipe is inside the coil and also when pipe is not present. It can be seen that for the scenario where pipe is not inside the coil, the magnetic field reduces from its maximum to zero between 0.202 and 0.218 seconds as shown in those labelled "Air" in Figure 3. When the pipe is present inside the coil (those curves labelled pipe in Figure 3), it can be seen that the magnetic field reduces more slowly with time and can still be detected at 0.25ms. Note that, at the same times, the field with the pipe present is initially smaller than the magnetic field in air, and it later forms a magnetic field in the opposite direction when the current is turned off. This latter magnetic field is due to the induced eddy currents, which continue to flow in the pipe after the current is switched off, until dissipated by the resistance of the pipe. It is also noted that the field is strongest under the conductor.

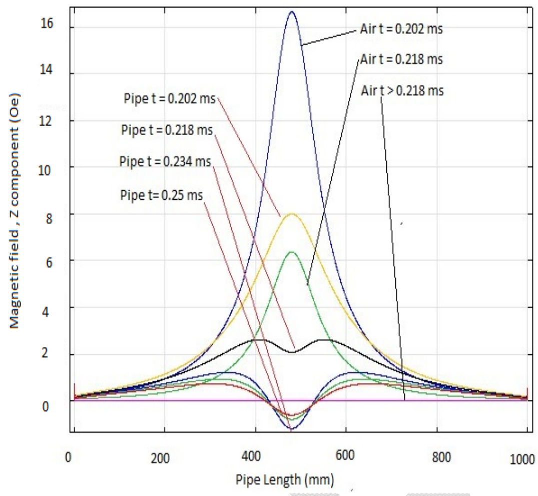


**Figure 3. Magnetic field along the longitudinal surface of the pipe**

### 1.1.1 PEC signals for detection of a pipe through various coverings

The magnetic field produced at a sensor outside the covering with different covering materials will exhibit different kinds of responses to the PEC stimulation as the magnetic field of the driver coil interacts with them. In order to better understand the effects of a specific covering on the PEC signal, the model was solved for different covering materials.

Previously W.Cheng [1], investigated these scenarios with a surface type probe, however the use of an encircling probe to produce the magnetic fields for PEC has not been studied. Therefore these simulations studied the encircling coil pulsed eddy current system. This was to investigate the effect of a larger uniform magnetic field generated around the circumference of the pipe. The material properties used in the model can be found in Table 3.

**Table 3. Material properties used in the models**

| Test object | Type | Conductivity (σ) [S/m] | Relative Pertmeability (μ) | Thickness [mm] |
|---|---|---|---|---|
| Stainless Steel | Covering | $1.3 \times 10^{6}$ | 1 | 0.5 |
| Galvanised Steel | Covering | $13 \times 10^{6}$ | 100 | 0.7 |
| Aluminium | Covering | $38 \times 10^{6}$ | 1 | 0.7 |
| Air | Covering | 1 | 0 | 0.7 |
| Insulation | Insulation | 1 | 0 | 50 |
| Carbon steel | Pipe wall | $4.25 \times 10^{6}$ | 1000 | 14 |
| Interior of the pipe | --- | 0 | 1 | --- |

The input excitation current used for exciting the coil as shown in Figure 2 was turned on at t=0 and reaches its maximum of I=28 Amps at t=0.202 ms when it was turned off and returned to zero sharply.

Figure 4 shows the time domain of the magnetic field Z component at the sensor point. These are presented for the coil around the covering in Figure 4(a) and coil around both pipe and covering in Figure 4 (b). The magnitude of the changes caused by the presence or absence of the pipe in the magnetic field distribution is difficult to see in these figures. .To better visualize the change of the field with and without the pipe it is helpful to subtract the two signals from each other. Data acquisitions are performed on two different models, one for coil around the covering and one for the coil around the covering and pipe. The differential magnetic field was mathematically defined as follows:

$$\nabla B_z = B_z \text{ pipe} - B_z \text{ air}$$

Where $B_z$ Pipe is the magnetic field of the coil around both covering and pipe, and $B_z$ air is the one only relating to the coil around covering. Bz is measured (ie a sensor is assumed) at a point between the coil and the covering.

Figure 5 (a) and (b) shows the differential time domain results for all covering materials. It is observed from these results that the differences between these 2 extreme cases of when pipe is inside the coil and when pipe is not inside the coil occur later in time domain for more conductive and permeable material.

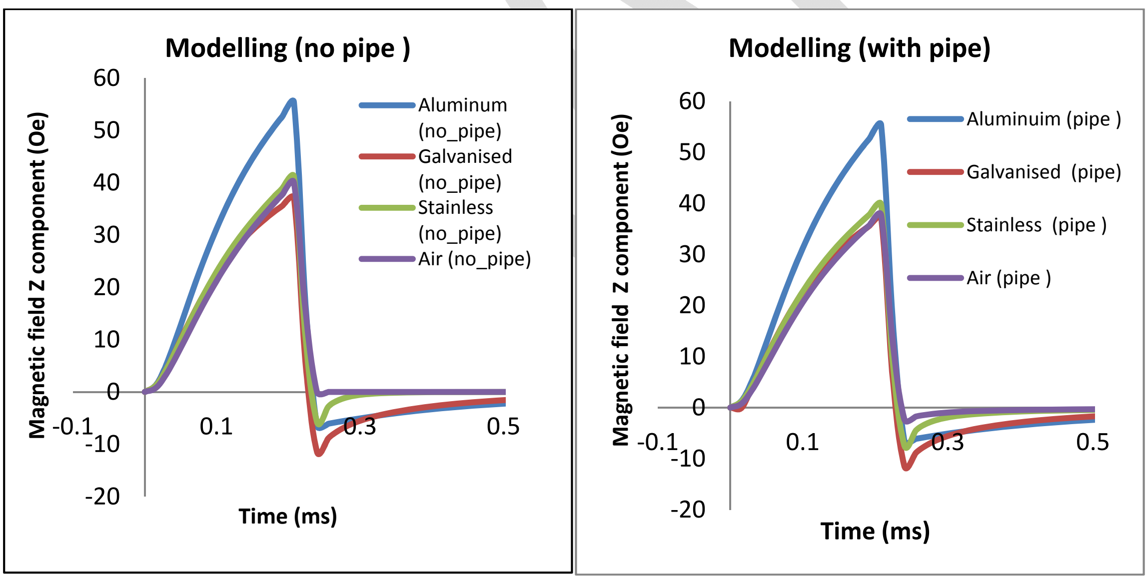


**Figure 4. Time responses of the magnetic field Z component (a) without the pipe (b) with the pipe**

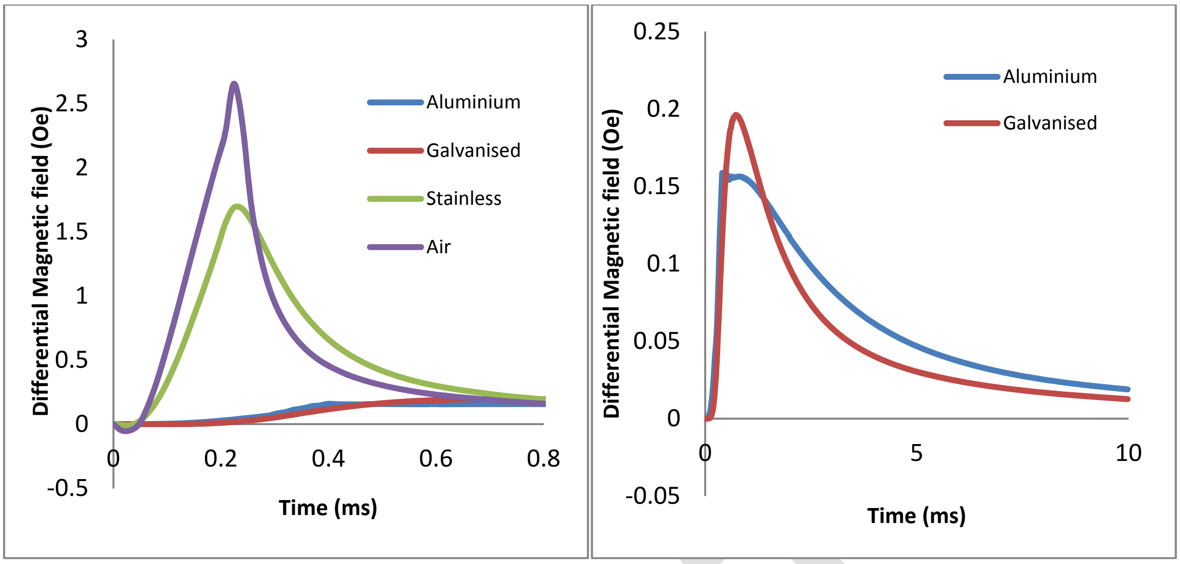


**Figure 5. Differential magnetic field signals (difference between pipe and no pipe for (a) all coverings (b) Aluminium and Galvanised steel covering**

As it was also expected and confirmed with the simulation results, the magnitudes of the magnetic field differences are larger for air (no metallic covering) than for all other coverings. The differential signals show the delay in the diffusion of the field caused by the high permeability and conductivity of galvanized steel and aluminium respectively. It is due to the concentration of the magnetic field on the surface of the covering and generation of eddy current on the covering. Note that this analysis ignores the possible effect of magnetisation of the galvanised steel.

## 1.2 *External Pipe wall thinning study under a specific covering*

The models were solved for different thicknesses of the pipe wall under a specific covering material. Material properties and dimensions used in these models are the same as those presented in Table 3. External thinning has been studied because this corresponds to the corrosion under insulation problem.

### 1.2.1 Uniform wall thinning with no covering

In order to establish a general relationship between the wall thinning and the magnetic field changes, outside wall thinning when there is no covering is studied first. In this study, the thickness of the wall of the pipe is reduced from outside and the magnetic field is captured at the sensor point. To improve the resolution of signals, test signals for different wall thicknesses were subtracted from a reference signal. The reference signal was considered to be the magnetic field signal found from a 14 mm thick wall and test signals were the magnetic field of different wall thicknesses (with material taken away from the outside).
Figure 6 shows the magnetic field at the position of the sensor where outside wall thinning was studied. Since the finite element analysis is highly mesh dependent, it was important to consider the changes that may occur due to the distribution of the mesh elements which happens when the geometry changes. In order to overcome this issue in solving these

models, whenever the wall thickness was varying, the pipe wall was layered appropriately and the material of the removed layer was changed to air.

These simulation results show that the magnitude of the differential signal is increasing as the thickness of the pipe reduces. Technically we can understand the differential pulse is proportional to the induced eddy currents in the pipe wall, because the effect of excitation magnetic field and the magnetic field of the eddy currents in a 14 mm thick wall is nullified by subtracting the two signals, only the effect of induced eddy current fields of the remaining wall thickness remain in the differential signal detected by the probe. This then causes the increase in the differential magnetic field as the wall thickness decreases. In these studies, it was observed that only the peaks of the differential signals are affected and signals do not cross zero.

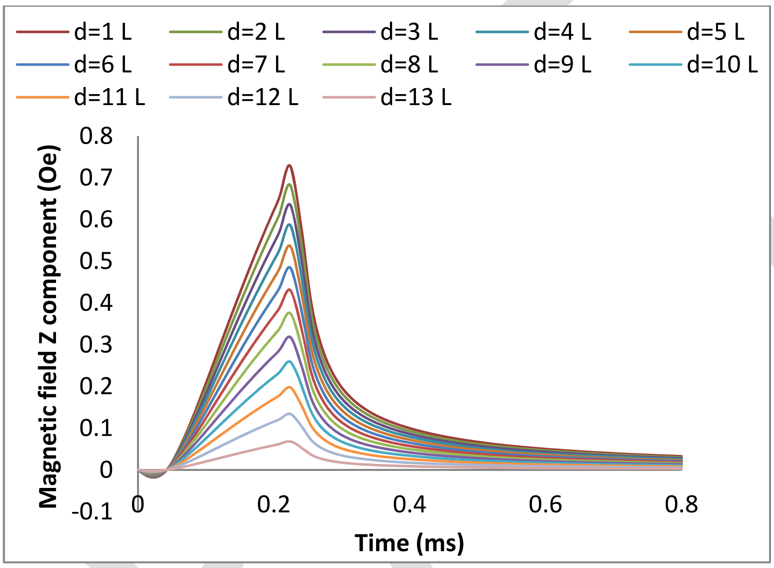


**Figure 6. Differential magnetic field for different external wall thickness changes**

### 1.2.2 Uniform wall thinning under stainless steel covering

Figure 7 shows the time domain of the differential magnetic field signals for the different wall thicknesses when there is a 0.7 mm stainless steel covering outside the nonconductive insulation. It can be seen that the same pattern is followed as when there was no covering present in the previous section.

Since stainless steel is an electrically conductive material it can act as a shield to an alternating magnetic field penetration to a great extent. It also means that the eddy currents will also be induced on the stainless steel covering. By choosing a reference signal which is the signal from a 14 mm pipe under the covering, the effects of such fields are nullified in subtraction and the remaining magnetic field affects can be related to those generated by the eddy currents in the pipe. This however means that the magnitude of the signals will be greatly attenuated.

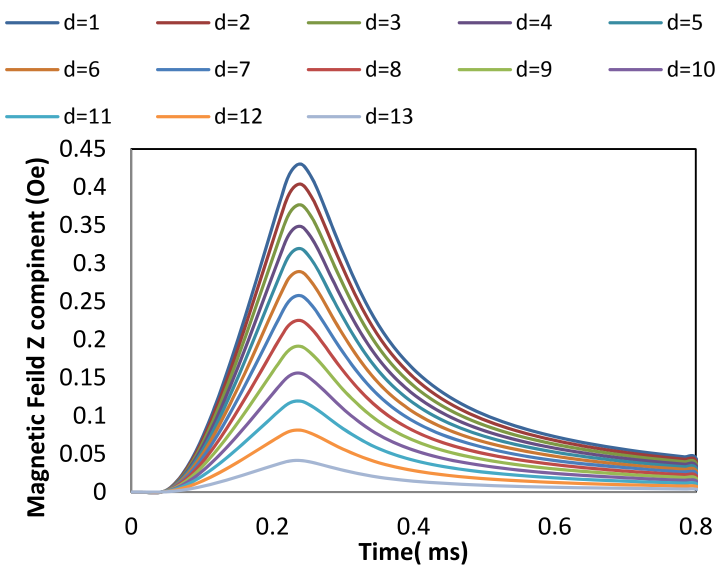


**Figure 7. Differential magnetic field signals for different pipe wall thickness under stainless steel covering**

### 1.2.3 Uniform wall thinning under Aluminium covering

Time domain signals of the differential signals under aluminium covering are shown in Figure 8. Since it was established that the changes in the magnetic field occur later in time for aluminium, simulations were run for longer time to capture the signals accordingly.

Like previous sections, a reference signals was chosen to nullify the effects of the eddy currents magnetic field in the covering and the one generated initially by the coil. This was the signal from the 14 mm pipe wall under the 0.7 mm aluminium covering. Since aluminium is about 3 times more conductive than stainless steel, the changing magnetic field is highly attenuated by the covering. As can be seen in the time domain signals the magnetic field changes happen later in time. The magnitudes of the differential signals are very low in comparison to the signals obtained in air and with stainless coverings. The modelling result indicates that the magnitude of the changes is very small, and this helps to determine either the sensitivity requirement of the sensors or the power needed into the system to provide a measurable output

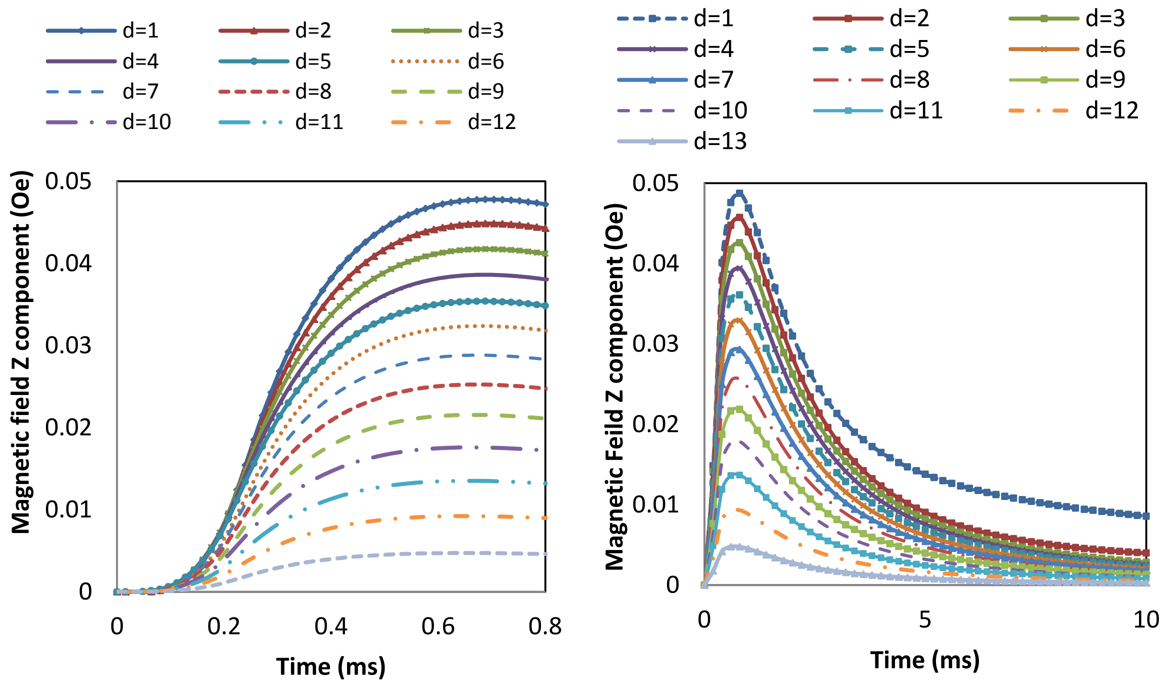


**Figure 8. Differential time domain signals under aluminium covering a) shorter time b) for a longer period of time**

### 1.2.4 Uniform wall thinning under galvanised steel covering.

Time domains of the differential signals under galvanised steel covering are shown in Figure 9. A reference signals was chosen to reduce the effects of the eddy current magnetic field in the covering and the one generated by the driver coil. The reference signal was the signal the signals obtained from the 14 mm pipe wall under the 0.7 mm galvanised covering. Since galvanised steel is conductive and also permeable, the magnetic field is highly weakened in passing through the covering.

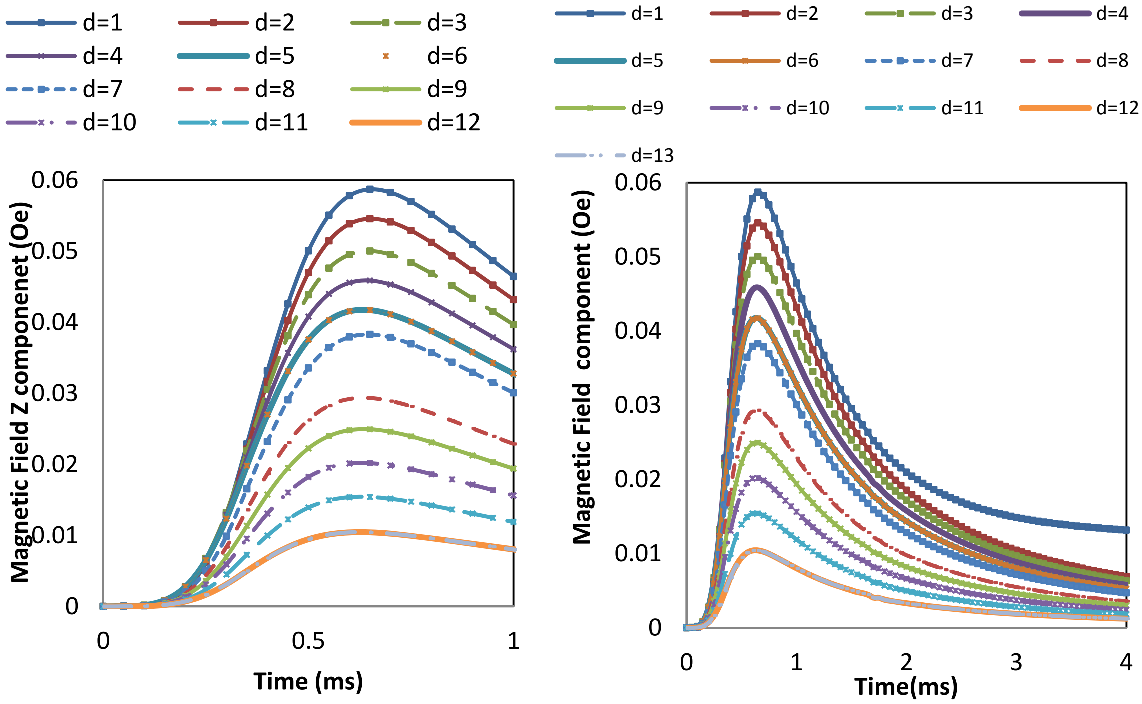


**Figure 9. Differential time domain response to pipe wall thinning under galvanised steel covering**

## 1.3 *Conclusion*

The PEC investigations performed in this paper illustrated the different PEC testing technique responses for the characterisation of wall thinning under insulation and conductive covering using an encircling probe. The investigations were carried out using finite element modelling and employing COMSOL multiphysics.

It was observed that as the covering becomes more conductive and or more magnetically permeable, the magnetic field generated by the driver coil takes longer to penetrate the covering and reach the pipe under the insulation.

The time domain differential signals were discussed for uniform wall thinning under each specific covering. It was found that the amplitude of the differential signals in time domain is affected by the uniform wall thinning.

# 2 Bibliography

[1] W. Cheng, "Pulsed Eddy Current Testing of Carbon Steel Pipes' Wall-thinning Through Insulation and Cladding," *Nondestruct Eval,* vol. 31, p. 215–224, 2012.

[2] "Industrial NDT," [Online]. Available: http://industrialndt.com/index.html. [Accessed 25 5 2015].

[3] A. Sophian, G. Y. Tian, D. Taylor and J. Rudlin, "A Feature Extraction Tehnique Based on Pincipal Cmponent Aalysis for pulsed Eddy current NDT," *NDT and E International,* vol. 36, no. 1, pp. 37-41, 2003.

[4] A. Sophian, Characterisation of Surface and Sub-Surface Discountinuities in Materials Using Pulsed Eddy Current Sensors, PhD Thesis, 2003, pp. 46-51.

[5] V. K. Babbar, P. R. Underhill, C. Stott and T. W. Krause, “Finite element modeling of second layer crack detection in aircraft bolt holes with ferrous fasteners presen,” *NDT&E International,* vol. 65, pp. 64-71, 2013.

[6] O. Biro and K. Preis , “On the use of the magnetic vector potential in the finite element analysis of three-dimensionaleddy currents,” *IEEE Transactions on Magnetics,* vol. 25, no. 4, pp. 3145-3159, 1989.

[7] J. Bowler, “Prediction and analysis of transient eddy-current probe signal,” *Rev. Progr. Quant. Nondestruct. Eval,* vol. 9, pp. 287-293, 1990.

[8] S. Majidnia, J. Rudlin and R. Nilavalan, “Investigation of an Encircling Pulsed Eddy Current probe for corrosion detection,” in *IEEE Conference Publications*, Valencia, Spain, 2014.

[9] Z. Abidin, *Modelling and experimental investigation of eddy current distribution for angular defect characterisation,* School of Electrical, Electronic and Computer Engineering: PhD thisis , 2010.